

ORIGINAL ARTICLE

Evaluation of k-Means and fuzzy C-means segmentation on MR images of brain



S. Madhukumar ^{a,*}, N. Santhiyakumari ^b

^a School of Electronics, St. Joseph's College of Engg. & Technology, Palai, Kerala 686 579, India

^b Department of Electronics & Communication, Knowledge Institute of Technology, Tamil Nadu, India

Received 17 September 2014; accepted 21 February 2015

Available online 24 March 2015

KEYWORDS

Glioblastoma multiforme;
Necrotic focus;
Vasogenic edema;
Bilateral filter;
Contrast limited adaptive
histogram equalization

Abstract This paper does the qualitative comparison of Fuzzy C-means (FCM) and k-Means segmentation, with histogram guided initialization, on tumor edema complex MR images. The accuracy of any segmentation scheme depends on its ability to distinguish different tissue classes, separately. Hence, there is a serious pre-requisite to evaluate this ability before employing the segmentation scheme on medical images. This paper evaluates the ability of FCM and k-Means to segment Gray Matter (GM), White Matter (WM), Cerebro-Spinal Fluid (CSF), Necrotic Focus of Glioblastoma Multiforme (GBM) and the perifocal vasogenic edema from pre-processed T1 contrast axial plane MR images of tumor edema complex. The experiment reveals that FCM identifies the vasogenic edema and the white matter as a single tissue class and similarly gray matter and necrotic focus, also. k-Means is able to characterize these regions comparatively better than FCM. FCM identifies only three tissue classes whereas; k-Means identifies all the six classes. The experimental evaluation of k-Means and FCM, with histogram guided initialization is performed in Matlab[®].

© 2015 The Authors. The Egyptian Society of Radiology and Nuclear Medicine. Production and hosting by Elsevier B.V. This is an open access article under the CC BY-NC-ND license (<http://creativecommons.org/licenses/by-nc-nd/4.0/>).

1. Introduction

Image segmentation is one of the most interesting and challenging problems in computer vision generally and medical imaging applications specifically. Segmentation partitions an image area or volume into nonoverlapping, connected regions, being homogeneous with respect to some signal characteristics (1). Segmentation approaches are subject to multiple

challenges stemming from image noise, image inhomogeneities, image artifacts such as partial volume effect, and discontinuities of boundaries due to similar visual appearance of adjacent brain structures. A variety of segmentation techniques have been developed to address these challenges. Brain MR segmentation methods can be classified into three main categories: probabilistic and statistical-based, atlas-based, and deformable model-based techniques (2). Hence, there is a mandatory prerequisite to investigate the ability of the segmentation scheme to characterize the complete tissue classes, present in the image, separately, before employing any statistical segmentation frame work. MR images of tumor edema complexes exhibit homogenous intensity features

* Corresponding author. Tel.: +91 9495431623.

E-mail address: madlekarthi@gmail.com (S. Madhukumar).

Peer review under responsibility of Egyptian Society of Radiology and Nuclear Medicine.

<http://dx.doi.org/10.1016/j.ejrnmm.2015.02.008>

0378-603X © 2015 The Authors. The Egyptian Society of Radiology and Nuclear Medicine. Production and hosting by Elsevier B.V. This is an open access article under the CC BY-NC-ND license (<http://creativecommons.org/licenses/by-nc-nd/4.0/>).

between WM and edema and similarly between necrotic focus and GM, as evident in Fig. 1. This is an investigation of the ability of FCM and k-Means to characterize the GM, WM, CSF, necrotic focus, vasogenic edema and background present in pre-processed axial plane T1 contrast MR images of GBM-edema complex.

Wen and Celebi (3) compared hard C-means and FCM clustering for color quantization. The results demonstrate that FCM is significantly slower than hard C-means, and that with respect to output quality, the former algorithm is neither objectively nor subjectively, superior to the latter.

Panda et al. (4) tested the performances FCM and k-Means. Two distance measures such as Manhattan (MH) and Euclidean (ED) are used to note how these distance measures influence the overall clustering performance. The performance has been compared based on seven parameters, sensitivity, specificity, precision, accuracy, run time, average intra cluster distance and inter cluster distance. Based on the experimental results, the paper concluded that both k-Means and FCM performed well.

However, k-Means outperformed FCM in terms of computational efficiency. FCM-MH combination produced most compact clusters, while k-Means-ED yielded most distinct clusters.

In Etehadtavakol et al. (5), two color segmentation techniques, k-Means and FCM for color segmentation of infrared (IR) breast images are modeled and compared. k-Means algorithm generated empty clusters. The fuzzy nature of IR breast images helps the FCM segmentation to provide more accurate results with no empty cluster.

Yin et al. (6) is a comparison of k-Means and FCM performance for automated determination of the Arterial Input Function (AIF). The results demonstrate that k-Means analysis can yield more accurate and robust AIF results, although it takes longer to execute than the FCM. Authors consider that this longer execution time is trivial relative to the total time required for image manipulation in a PACS setting, and is acceptable if an ideal AIF is obtained. Therefore, the literature suggested, the k-Means method is preferable to FCM in AIF detection.

Sueli et al. (7) presented a comparison among non-hierarchical and hierarchical clustering algorithms including SOM (Self-Organization Map) neural network and FCM. Data were simulated, considering correlated and uncorrelated

variables, non-overlapping and overlapping clusters with and without outliers. A total of 2530 data sets were simulated. The results showed that FCM had a very good performance in all cases being very stable even in the presence of outliers and overlapping. All other clustering algorithms were very affected by the amount of overlapping and outliers. SOM neural network did not perform well in almost all cases being much affected by the number of variables and clusters. The traditional hierarchical clustering and k-Means methods presented similar performance.

In Ghosh and Dubey (8), centroid based k-Means and representative object based FCM clustering algorithms are compared. These algorithms are applied and performance is evaluated on the basis of the efficiency of clustering output. The numbers of data points as well as the number of clusters are the factors upon which the behavior patterns of both the algorithms are analyzed. Literature observed FCM produces close results to k-Means clustering but it still requires more computational time than k-Means.

Wang and Garibaldi (9) applied k-Means and FCM to cluster a lymph node tissue section which had been diagnosed with metastatic infiltration. Each cluster algorithm was run 10 times as different initialization states may lead to different clustering results. The performance of the two algorithms was compared by subjectively altering the number of clusters from 2 to 9 and analyzed the results using false-color images which are produced as a function of the spatial coordinates on the tissue section. In the initial stages of this experiment, it was observed that the ranges of the first three principal components were too small and may lead to small objective function values in FCM. Therefore, the minimal amount of improvement must be set to a small enough value to allow the cluster center positions to improve; otherwise the iteration will stop prematurely. After adjusting this setting, the performance of FCM was significantly better. The results show that FCM can separate the major different tissue types using just a small number of clusters, whereas k-Means is only able to separate them if a larger cluster number is used.

It seems the segmentation accuracy of FCM and k-Means is image dependent. The literatures are not unanimous regarding their opinion about the performance of k-Means and FCM. This paper proceeds through the specification of test images, preprocessing, mathematical formulation of k-Means and FCM. Eventually, qualitative evaluation of segmentation results of both the algorithm, in terms of number of tissue classes identified and the accuracy of clustering are furnished.

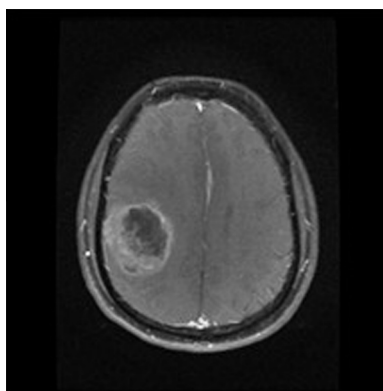


Fig. 1 Axial plane T1 contrast MRI of GBM-edema complex. (Image Courtesy: Hind Labs, Kottayam Medical College Kerala).

2. Materials and methods

Axial Plane T1 contrast enhanced (Series: AX T1 SE FS + C, Spin Echo Sequence (SE)) MR images (courtesy: Hind Labs, Govt. Medical College Kottayam, Kerala) were selected for the experimental evaluation of k-Means and FCM. The specification of MR equipment is; Manufacturer: GE Medical Systems, Model Name: Signa HDxt, Acquisition Type: 2D and 1.5T field strength. Experimental evaluation of FCM and k-Means was performed on Matlab®, (Version: 7.12.0.635 (R2011a)) Image Processing Tool Box. The preprocessing includes elimination of noisy background, restoration with bilateral filter (10) contrast enhancement with Contrast Limited Adaptive Histogram Equalization (CLAHE) (11)

and skull stripping. Fig. 2 shows the output images at various stages of preprocessing. FCM (12) is based on minimizing an objective function, with respect to fuzzy membership ‘ U ’, and set of cluster centroids, ‘ V ’.

$$J_m(U, V) = \sum_{j=1}^N \sum_{i=1}^C u_{ij}^m d^2(x_j, v_i) \quad (1)$$

In (1) $X = \{x_1, x_2, \dots, x_j \dots x_N\}$ is a $p \times N$ data matrix, where, p represents the dimension of each x_j ‘feature’ vector, and N represents the number of feature vectors (pixel numbers in the image). ‘ C ’ is the number of clusters. $U_{ij} \subseteq U(p, N, C)$ is the membership function of vector x_j to the i th cluster, which satisfies $u_{ij} \in [0, 1]$ and,

$$\sum_{i=1}^C u_{ij} = 1, \quad j = 1, 2, \dots, N \quad (2)$$

The membership function can be expressed as,

$$u_{ij} = \frac{1}{\sum_{k=1}^C \left(\frac{d(x_j, v_i)}{d(x_j, v_k)} \right)^{2/m-1}} \quad (3)$$

$V = \{v_1, v_2 \dots v_i \dots v_C\}$ is a $p \times C$ matrix and denotes the cluster feature center.

$$v_i = \frac{\sum_{j=1}^N (u_{ij})^m x_j}{\sum_{j=1}^N (u_{ij})^m} \quad i = 1, 2 \dots C \quad (4)$$

$m \in (1, \infty)$ is a weighting exponent on each fuzzy membership, which controls the degree of fuzziness. $d^2(x_j, v_i)$ is a measurement of similarity between x_j and v_i .

$$d^2(x_j, v_i) = \|x_j - v_i\|^2 \quad (5)$$

$\|\cdot\|$ can be either Euclidean distance or one of its generalizations as Mahalanobis distance. Euclidian metric is used in this

experimental study. Degree fuzziness was set to two. It was observed that variations in degree of fuzziness did not have substantial influence on segmentation outcome. The feature vector ‘ X ’ in the MR image represents the pixel intensities, so $p = 1$. ‘ C ’ is the number of tissue classes in the pre-processed MR image and cluster centers in ‘ V ’ are the mean intensity of tissue classes, derived from the histogram guided initialization. The FCM algorithm iteratively optimizes $J_m(U, V)$ with the continuous update of ‘ U ’ and ‘ V ’, until $|U^{(l+1)} - U^{(l)}| \leq \epsilon$ where, ‘ l ’ is the number of iterations and ‘ ϵ ’ is the user defined threshold or termination criteria. ‘ ϵ ’ was set to 0.001 in this experiment. The number of tissue classes ‘ C ’ is six, GM, WM, CSF, necrosis, enhancing edema and background as visible in Figs. 3 and 4. The CSF is absent in the axial slice shown in Fig. 5 so that the number of tissue classes is five.

The mean intensity of tissue classes for initializing both FCM and k-Means is derived from a histogram guided method. In histogram guided initialization, let μ be the vector of mean intensity of ‘ k ’ tissue classes present in the pre-processed image,

$$\mu = \{\mu_1, \mu_2, \mu_3 \dots \mu_k\} \quad (6)$$

and ‘ j ’ be an arbitrary sequence

$$j = \{0, 1, 2, 3 \dots k\} \quad (7)$$

The range of pixel intensities or the interval between maximum and minimum intensities in the pre-processed MR image is divided into ‘ k ’ intensity bins, with $k + 1$ intensity points between the maximum and minimum intensity. These intensity points,

$$I_j = I_L + j \left(\frac{I_H - I_L}{k} \right) \quad (8)$$

where I_H is the maximum intensity in the pre-processed MR image and I_L , the minimum intensity. As pointed earlier, the

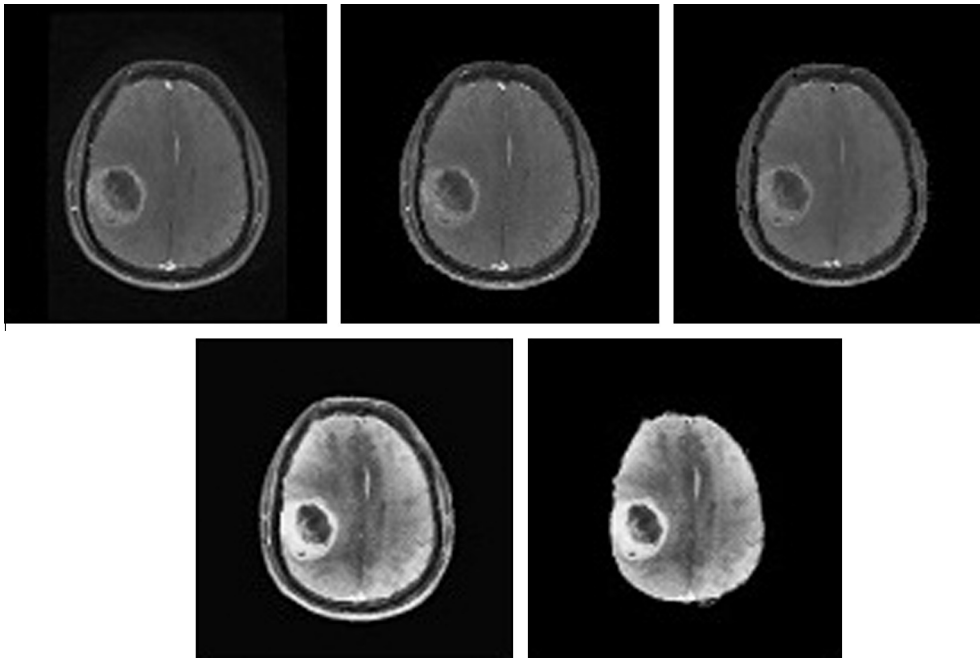


Fig. 2 Original image, background eliminated image, restored image after bilateral filtering, contrast enhanced image after CLAHE and skull stripped image.

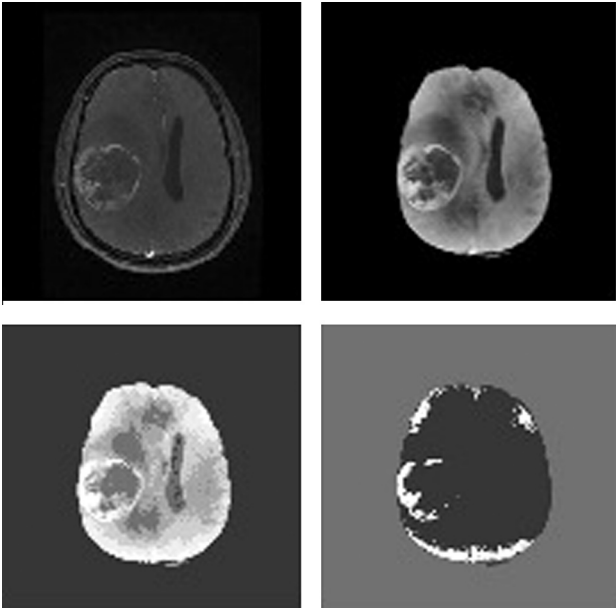


Fig. 3 Raw MR image 1 preprocessed image, clustered classes with k-Means and clustered classes with FCM.

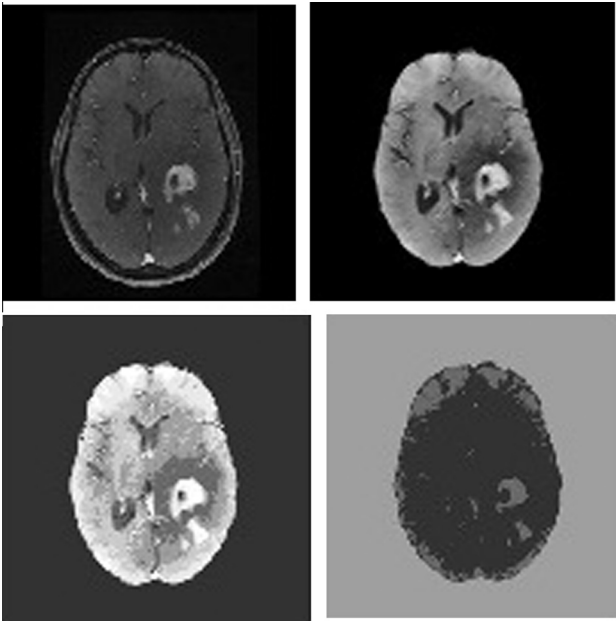


Fig. 4 Raw MR image 2 preprocessed image, clustered classes with k-Means and clustered classes with FCM.

number of tissue classes ‘k’ is six, GM, WM, CSF, necrosis, enhancing edema and background.

$$\mu_j = \frac{\sum_{i=j}^{j+1} m_i}{\sum_{i=j}^{j+1} n_i} \quad (9)$$

The mean of pixel intensities present in a bin represents the mean intensity of tissue class corresponding to that bin. ‘ i ’ is the intensities present in the j th bin and n_i is the histogram of these intensities.

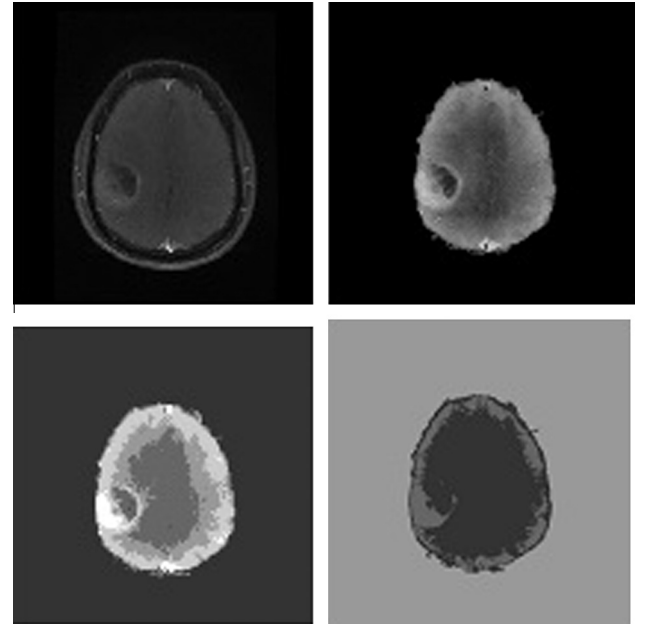


Fig. 5 Raw MR image 3, preprocessed image, clustered classes with k-Means and clustered classes with FCM.

In k-Means clustering (13), let the initialized cluster centers at the first iteration be,

$$\mu(1) = \{\mu_1(1), \mu_2(1), \mu_3(1), \dots, \mu_k(1)\} \quad (10)$$

The pixel intensities actually present in the pre-processed MR image are redistributed to one of the classes or clusters such that,

$$I \in C_j(1) \text{ if } \|I - \mu_j(1)\| < \|I - \mu_i(1)\| \quad (11)$$

where $I = 1, 2, 3, \dots, k$ and $j = 1, 2, 3, \dots, k$ but $i \neq j$ and C_j is the cluster or tissue class with class mean or cluster center μ_j . Generalizing (11), at the n th iterative step,

$$I \in C_j(n) \text{ if } \|I - \mu_j(n)\| < \|I - \mu_i(n)\| \quad (12)$$

Before the $(n + 1)$ th iteration, class means or cluster centers are updated, such that the sum of squared distances from all samples or intensities in the tissue class or cluster $C_j(n)$ to the cluster center is minimized. In fact, new cluster center is just mean intensity of the tissue class C_j ,

$$\mu_j(n+1) = \frac{1}{N_j} \sum_{I \in C_j(n)} I \quad j = 1, 2, 3, \dots, k \quad (13)$$

where N_j is the number of samples in the cluster C_j at n th iteration $C_j(n)$ otherwise N_j is the number of intensities in the j th tissue class in the pre-processed MR image. The algorithm converges when the condition (14) is satisfied and tissue class mean updating would be terminated.

$$\mu_j(n+1) = \mu_j(n) \quad \forall j = 1, 2, 3, \dots, k \quad (14)$$

After the class mean recalculation has been converged, intensities in the image is redistributed to one of the clusters, obeying (12), so that the output mask contains tissue class labels from one to k .

3. Results and discussion

The ability of k-Means and FCM to classify the tissue classes present in the real MR images is qualitatively analyzed. The first raw MR image, pre-processed image, clustered image with k-Means and FCM, respectively are showed in Fig. 3. Figs. 4 and 5 correspond to second and third test images. First test image in Fig. 1 and second one in Fig. 2 contain five tissue types and background. The morphological structures present in first and second test images are WM, GM, CSF, necrotic focus and edema. But, CSF is absent in the third test image.

From Figs. 3–5 it is apparent that FCM is able to identify only three classes, including the background, in all the test images. FCM consider edema and certain parts of WM as a single tissue class. Similarly, FCM clubs GM, CSF and necrotic focus into a single tissue class. In other words, FCM produces empty clusters. Even if the k-Means identifies all the tissue classes, certain parts of WM are clubbed with vasogenic edema because of their homogenous intensity features. This happens to certain regions of necrotic focus, CSF and GM also. Perhaps, semi-automated methods like deformable model based segmentation may be considered as an alternative technique. In deformable model based techniques, a rough margin of the Region of Interest (ROI) is marked manually so that there is no burden of identifying distinct classes present in the image to be processed.

4. Conclusion

The efficacy of FCM and k-Means, with histogram guided initialization, was analyzed on T1 contrast axial plane MR images of GBM-edema complex. FCM could identify two tissue classes and background. It merged GM, CSF and necrotic focus into one class and WM and perifocal edema into another. FCM produced three empty clusters in first two test images and two in the last one. k-Means could identify CSF, GM, WM, necrosis, edema and background region. But, certain parts of the WM were clustered with enhancing edema and vice versa. This cross talk occurs between CSF, necrosis and GM also. This happens as the intensity features of the edema and certain parts of WM are perfectly equal. Similarly, certain parts of CSF, GM and necrosis also shares homogenous intensity features. Fully automated segmentation of GBM, hence would be intricate and intensity based segmentation would not be viable for MR images of GBM-edema complex.

Conflict of interest

None.

Acknowledgement

The authors would like to thank Dr. Jose Tom, Professor & Head, Department of Radiotherapy, Government Medical College, Kottayam, Kerala, Dr. Unni. S. Pillai, Department of Oncology, The Jawaharlal Institute of Postgraduate Medical Education & Research (JIPMER), Puducherry and Dr. GowriShanker, Hindlab, Govt. Medical College, Kottayam, for their incessant involvement in this endeavor.

References

- (1) Elnakib A, Gimel'farb G, Suri JS, El-Baz A. Medical image segmentation: a brief survey. Handbook of multi modality state-of-the-art medical image segmentation and registration methodologies, vol. 2(1). New York: Springer-Verlag; 2011. p. 1–39.
- (2) Alansary A, Soliman A, Khalifa F, Elnakib A, Mostapha M, Nitzken M, et al. MAP-based framework for segmentation of MR brain images based on visual appearance and prior shape. MIDAS J 2013;1:1–13, <<http://hdl.handle.net/10380/3440>> .
- (3) Wen Q, Celebi ME. Hard versus fuzzy c-means clustering for color quantization. EURASIP J Adv Signal Process 2011;2011: 118.
- (4) Panda S, Sahu S, Jena P, Chattopadhyay S. Comparing fuzzy-C means and K-means clustering techniques: a comprehensive study. Adv Intell Soft Comput 2012;166:451–60.
- (5) Etehadtavakol M, Sadri S, Ng EY. Application of K- and fuzzy c-means for color segmentation of thermal infrared breast images. J Med Syst Arch 2010;34:35–42.
- (6) Yin J, Sun H, Yang J, Guo Q. Comparison of K-means and fuzzy c-means algorithm performance for automated determination of the arterial input function. PLoS One 2014;9(2):e85884.
- (7) Mingoti Sueli A, Lima Joab O. Comparing SOM neural network with Fuzzy c-means, K-means and traditional hierarchical clustering algorithms. Eur J Oper Res 2006;174:1742–59.
- (8) Ghosh S, Dubey SK. Comparative analysis of K-means and fuzzy C-means algorithms (IJACSA). Int J Adv Comput Sci Appl 2013;3:45–7.
- (9) Wang XY, Garibaldi JM. A comparison of fuzzy and non-fuzzy clustering techniques in cancer diagnosis; 2005 <<http://ima.ac.uk/papers/wang2005.pdf>> .
- (10) Tomasi C, Manduchi R. Bilateral filtering for gray and color images. In: Proceedings of the 1998 IEEE international conference on computer vision. Bombay, India; 1998.
- (11) Zuiderveld Karel. Contrast limited adaptive histogram equalization. Graphic Gems IV. San Diego: Academic Press; 1994, p. 474–85.
- (12) Shen S, Sandham W, Granat M, Sterr A. MRI fuzzy segmentation of brain tissue using neighborhood attraction with neural-network optimization. IEEE Trans Inform Technol Biomed 2005;9:459–67.
- (13) Ray S, Turi RH. Determination of number of clusters in K-means clustering and application in colour image segmentation. In: Proc 4th international conference on advances in pattern recognition and digital techniques (ICAPRDT'99). Calcutta, India; 1999. p. 137–43.